

Quantum transport signatures of non-trivial topological edge states in a ring-shaped Su-Schrieffer-Heeger double-chain system

Cheng-Zhi Ye(叶成芝), Lan-Yun Zhang(张蓝云), and Hai-Bin Xue(薛海斌)
Citation: Chin. Phys. B, 2022, 31 (**2**): 027304. DOI: 10.1088/1674-1056/ac34ff
Journal homepage: http://cpb.iphy.ac.cn; http://iopscience.iop.org/cpb

What follows is a list of articles you may be interested in

Pure spin-current diode based on interacting quantum dot tunneling junction

Zhengzhong Zhang(张正中), Min Yu(余敏), Rui Bo(薄锐), Chao Wang(王超), and Hao Liu(刘昊)
Chin. Phys. B, 2021, 30 (**11**): 117305. DOI: 10.1088/1674-1056/abfbd8

Goos-Hänchen-like shift related to spin and valley polarization in ferromagnetic silicene

Mei-Rong Liu(刘美荣), Zheng-Fang Liu(刘正方), Ruo-Long Zhang(张若龙), Xian-Bo Xiao(肖贤波), and Qing-Ping Wu(伍清萍)
Chin. Phys. B, 2021, 30 (**10**): 107302. DOI: 10.1088/1674-1056/ac1e16

Quantum transport through a Z-shaped silicene nanoribbon

A Ahmadi Fouladi
Chin. Phys. B, 2017, 26 (**4**): 047304. DOI: 10.1088/1674-1056/26/4/047304

Perfect GMR effect in gapped graphene-based ferromagnetic—normal—ferromagnetic junctions

Hossein Karbaschi, Gholam Reza Rashedi
Chin. Phys. B, 2015, 24 (**4**): 047305. DOI: 10.1088/1674-1056/24/4/047305

Temperature-controllable spin-polarized current and spin polarization in a Rashba three-terminal double-quantum-dot device

Hong Xue-Kun, Yang Xi-Feng, Feng Jin-Fu, Liu Yu-Shen
Chin. Phys. B, 2013, 22 (**5**): 057306. DOI: 10.1088/1674-1056/22/5/057306

Quantum transport signatures of non-trivial topological edge states in a ring-shaped Su–Schrieffer–Heeger double-chain system

Cheng-Zhi Ye(叶成芝)[1], Lan-Yun Zhang(张蓝云)[2], and Hai-Bin Xue(薛海斌)[2,†]

[1] *School of Physics and Electronic Engineering, Linyi University, Linyi* 276005, *China*

[2] *Key Laboratory of Interface Science and Engineering in Advanced Materials, Ministry of Education, Taiyuan University of Technology, Taiyuan* 030024, *China*

(Received 17 August 2021; revised manuscript received 8 October 2021; accepted manuscript online 1 November 2021)

In the ring-shaped Su–Schrieffer–Heeger (SSH) double-chain, the quantum interference between the two different electron tunneling paths of the upper and lower chains has an important influence on the electron transport properties of non-trivial topological edge states. Here, we have studied the electron transport signatures of non-trivial topological edge states in a ring-shaped SSH double-chain system based on the wave-guide theory and transfer-matrix method. In the ring-shaped SSH double-chain with the upper chain being different from the lower one, it is demonstrated that the electron transmission probability displays the four and two resonance peaks associated with the non-trivial topological edge states in the weak and strong coupling regimes, respectively. Whereas in the case of the upper chain being the same as the lower one, the two transmission resonance peaks associated with the non-trivial topological edge states in the weak coupling regime are only found, and that in the strong coupling regime disappear that originated from the destructive interference between the two different electron tunneling paths of the upper and lower chains. Consequently, the variation of the number of transmission resonance peaks associated with the non-trivial topological edge states in the weak and strong coupling regimes suggests that an alternative scheme for detecting non-trivial topological edge states in the ring-shaped SSH double-chain system.

Keywords: ring-shaped Su–Schrieffer–Heeger double-chain, non-trivial topological edge states, transmission probability

PACS: 73.23.–b, 73.20.–r, 71.23.An, 74.25.Jb **DOI:** 10.1088/1674-1056/ac34ff

1. Introduction

Non-trivial topological edge states have potential applications in spintronics and quantum computation because they have a strong robustness against local material defects and disorders.[1,2] The one-dimensional Su–Schrieffer–Heeger (SSH) chain,[3] which was originally used to describe polyacetylene molecule, is one of the simplest systems with non-trivial topological edge states. Particularly, the SSH models have been experimentally realised with the photonic lattices,[4–6] optical lattices,[7] engineered atomic chains[8,9] and microring array.[10] To realize quantum devices based on non-trivial topological edge states, how to detect the edge states is one of the important topics. Consequently, how to determine the existence of non-trivial topological edge states in the SSH chain systems has become an important topic in condensed matter physics.[11–23] Recently, it has been demonstrated that electron transport properties associated with non-trivial topological edge states can be used to determine the existence of the non-trivial topological edge states.[24–30] Compared with the SSH chains being of the topologically trivial and plain phases, the (Andreev) conductance and the shot noise of the topologically nontrivial chain in the zero-bias limit display an opposite odd–even parity effects.[26] In particular, the transport current and its Fano factor can be used to distinguish whether the SSH chain system is of the topologically non-trivial or trivial phases.[27,28] For example, in the vicinity of the zero energy, the variation of the number of transmission resonance peaks in the weak and strong coupling regimes can be used to detect whether the SSH chain is of the nontrivial topological state or not and determine the winding numbers of different nontrivial topological states.[29,30] Interestingly, in a ring-shaped SSH double-chain system, which is contrary to the two coupled SSH double chains,[16,17,30] the conduction electrons from the source electrode have two different paths through the SSH system and tunnel into the drain electrode. In this case, the two different electron tunneling paths can exhibit the quantum interference effect. However, the influence of the quantum interference between the two different electron tunneling paths on the electron transport properties of non-trivial topological edge states in a ring-shaped SSH double-chain system has not yet been revealed.[31–36]

In this paper, we study the electron transport signatures of non-trivial topological edge states in a ring-shaped SSH double-chain system, and discuss the dependence of the electron transport properties of edge states on the quantum interference between the two different electron tunneling paths of the upper and lower chains. In the case of the upper chain being different from the lower one, the four and two trans-

†Corresponding author. E-mail: xuehaibin@tyut.edu.cn

© 2022 Chinese Physical Society and IOP Publishing Ltd

mission resonance peaks associated with the non-trivial topological edge states in the weak and strong coupling regimes can be found, respectively. Whereas in the case of the upper chain being the same as the lower one, the number of the transmission resonance peaks in the weak coupling regime is only two, and the two transmission resonance peaks in the strong coupling regime will disappear that originating from the destructive interference between the two different electron tunneling paths of the upper and lower chains. Importantly, the number of the corresponding transmission resonance peaks in the strong coupling regime is also reduced by two. Therefore, with increasing the strength of tunneling coupling between the ring-shaped SSH double-chain and the two external electrodes from the weak to the strong coupling regimes, the non-trivial topological edge states can be detected by observing the variation of the number of transmission resonance peaks associated with the non-trivial topological edge states in the vicinity of the zero energy.

The paper is organized as follows. In Section 2, we introduce the ring-shaped SSH double-chain system, and outline the procedure to calculate the transmission probability of electron transport through the ring-shaped SSH double-chain system based on the wave-guide theory and transfer-matrix method. The numerical results are discussed in Section 3, where we first discuss the topological properties of the non-trivial edge states of the SSH single-chain, and then study the influence of the quantum interference between the two different electron tunneling paths of the upper and lower chains on the electron transport properties of non-trivial topological edge states in the ring-shaped SSH double-chain system, and suggest an alternative scheme for detecting its non-trivial topological edge states. Finally, in Section 4 we summarize the work.

2. Model and formalism

2.1. The ring-shaped SSH double-chain system

The ring-shaped SSH double-chain, which consists of the two SSH chains connected in parallel to two leads, see Fig. 1(a), is described by the Hamiltonian

$$\begin{aligned} H_{\text{SSH-ring}} = {} & \upsilon_1 \sum_{n=1}^{N_1} \left(d^{\dagger}_{1,n,B} d_{1,n,A} + d^{\dagger}_{1,n,A} d_{1,n,B} \right) \\ & + w \sum_{n=1}^{N_1-1} \left(d^{\dagger}_{1,n,B} d_{1,n+1,A} + d^{\dagger}_{1,n+1,A} d_{1,n,B} \right) \\ & + \upsilon_2 \sum_{m=1}^{N_2} \left(d^{\dagger}_{2,m,B} d_{2,m,A} + d^{\dagger}_{2,m,A} d_{2,m,B} \right) \\ & + w \sum_{m=1}^{N_2-1} \left(d^{\dagger}_{2,m,B} d_{2,m+1,A} + d^{\dagger}_{2,m+1,A} d_{2,m,B} \right). \end{aligned} \tag{1}$$

The first and second terms describe the upper SSH chain, and the third and fourth terms describe the lower SSH chain. Here, $d^{\dagger}_{1,n,\beta}$ ($d_{1,n,\beta}$) is the creation (annihilation) operator of an electron at β ($\beta = A, B$) sublattice in n-th cell of the upper chain of the ring-shaped SSH double-chain, υ_1 the intra-cell hopping amplitude of the upper chain and w inter-cell hopping one of the upper and lower chains; while in the case of the lower chain $i = 2$. N_1 and N_2 are the number of cells of the upper and lower chains, respectively.

The two leads are modeled as the Hamiltonian

$$H_{\text{L,lead}} = t_0 \sum_{j=-\infty}^{-1} \left(a^{\dagger}_j a_{j-1} + a^{\dagger}_{j-1} a_j \right), \tag{2}$$

$$H_{\text{R,lead}} = t_0 \sum_{j=1}^{\infty} \left(a^{\dagger}_j a_{j+1} + a^{\dagger}_{j+1} a_j \right), \tag{3}$$

where $a^{\dagger}_j$ (a_j) is the creation (annihilation) operator of an electron at j-th lattice in the leads, and t_0 the hopping amplitude between two nearest-neighbor lattices in the leads. The electron tunneling between the ring-shaped SSH double-chain and the two leads reads

$$\begin{aligned} H_{\text{tunneling}} = {} & t_{\text{L},1} a^{\dagger}_{-1} d_{1,1,A} + t_{\text{L},1} d^{\dagger}_{1,1,A} a_{-1} + t_{\text{R},1} a^{\dagger}_1 d_{1,N_1,B} \\ & + t_{\text{R},1} d^{\dagger}_{1,N_1,B} a_1 + t_{\text{L},2} a^{\dagger}_{-1} d_{2,1,A} + t_{\text{L},2} d^{\dagger}_{2,1,A} a_{-1} \\ & + t_{\text{R},2} a^{\dagger}_1 d_{2,N_2,B} + t_{\text{R},2} d^{\dagger}_{2,N_2,B} a_1, \end{aligned} \tag{4}$$

where $t_{\alpha,1}$ ($t_{\alpha,2}$) is the amplitude of electron tunneling between the α-lead and the upper (lower) chain of the ring-shaped SSH double-chain.

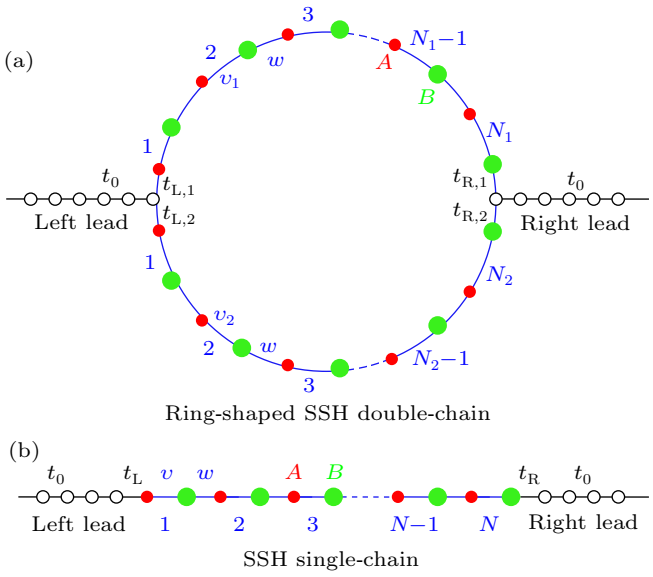


Fig. 1. Schematics of the considered ring-shaped SSH double-chain and the SSH single-chain systems coupled to the left (source) and right (drain) leads (electrodes). The hollow circles denote lattices on the leads, and red and green circles describe the sublattices A and B of the SSH chain, respectively. t_0 describes the hopping amplitude between the two nearest-neighbor lattices on the leads. (a) $t_{\alpha,1}$ ($t_{\alpha,2}$) characterizes the strength of tunneling coupling between the upper (lower) chain and the α-electrode, and υ_1 (υ_2) the intra-cell hopping amplitude of the upper (lower) chain, and w inter-cell hopping amplitude of the upper and lower chains. N_1 and N_2 are the number of cells of the upper and lower chains, respectively. (b) υ and w describe the intra-cell hopping amplitude and the inter-cell hopping amplitude of the SSH single-chain, respectively. t_α characterizes the strength of tunneling coupling between the SSH single-chain and the α-electrode, N denotes the number of cells of the SSH single-chain.

2.2. The transmission probability and transfer-matrix method

To calculate transmission probability of electron transport through the ring-shaped SSH double-chain, the wave-guide theory and transfer-matrix method are adopted in the following calculation. In the Wannier basis, the wave function of the total system $|\Psi\rangle$ can be expressed as

$$\begin{aligned}|\Psi\rangle = &\sum_{j=-\infty}^{-1} a_{j,k}|j\rangle + \sum_{j=1}^{\infty} a_{j,k}|j\rangle \\ &+ \sum_{n=1}^{N_1}\left(d_{1,n,A,k}|n,A\rangle + d_{1,n,B,k}|n,B\rangle\right) \\ &+ \sum_{m=1}^{N_2}\left(d_{2,m,A,k}|m,A\rangle + d_{2,m,B,k}|m,B\rangle\right), \end{aligned} \tag{5}$$

where the coefficients $a_{j,k}$ and $d_{1,n,\beta,k}$ ($d_{2,n,\beta,k}$) correspond to the probability amplitudes at j-th lattice in the leads and β sublattice in n-th cell of the upper (lower) chain of the ring-shaped SSH double-chain, respectively. Inserting Eq. (5) into the time-independent Schrödinger Equation $H|\Psi\rangle = E|\Psi\rangle$, by setting the coefficients of Wannier states on the left-hand side of the equation being equal to that on the right-hand side, the following set of coupled linear equations can be obtained as

$$t_0 a_{-2,k} + t_{\mathrm{L},1} d_{1,1,A,k} + t_{\mathrm{L},2} d_{2,1,A,k} = E a_{-1,k}, \tag{6}$$
$$\upsilon_1 d_{1,1,B,k} + t_{\mathrm{L},1} a_{-1,k} = E d_{1,1,A,k}, \tag{7}$$
$$\upsilon_1 d_{1,n,A,k} + w_1 d_{1,n+1,A,k} = E d_{1,n,B,k}, \quad 1 \le n \le N_1 - 1, \tag{8}$$
$$\upsilon_1 d_{1,n,B,k} + w_1 d_{1,n-1,B,k} = E d_{1,n,A,k}, \quad 2 \le n \le N_1, \tag{9}$$
$$\upsilon_1 d_{1,N_1,A,k} + t_{\mathrm{R},1} a_{1,k} = E d_{1,N_1,B,k}, \tag{10}$$
$$\upsilon_2 d_{2,1,B,k} + t_{\mathrm{L},2} a_{-1,k} = E d_{2,1,A,k}, \tag{11}$$
$$\upsilon_2 d_{2,m,A,k} + w_2 d_{2,m+1,A,k} = E d_{2,m,B,k}, \quad 1 \le m \le N_2 - 1, \tag{12}$$
$$\upsilon_2 d_{2,m,B,k} + w_2 d_{2,m-1,B,k} = E d_{2,m,A,k}, \quad 2 \le m \le N_2, \tag{13}$$
$$\upsilon_2 d_{2,N_2,A,k} + t_{\mathrm{R},2} a_{1,k} = E d_{2,N_2,B,k}, \tag{14}$$
$$t_0 a_{2,k} + t_{\mathrm{R},1} d_{1,N_1,B,k} + t_{\mathrm{R},2} d_{2,N_2,B,k} = E a_{1,k}. \tag{15}$$

Using transfer-matrix method, Eqs. (8)–(14) can be reexpressed as

$$\begin{pmatrix} a_{1,k} \\ d_{1,N_1,B,k} \end{pmatrix} = T_1 \begin{pmatrix} d_{1,1,A,k} \\ a_{-1,k} \end{pmatrix}, \tag{16}$$
$$\begin{pmatrix} a_{1,k} \\ d_{2,N_2,B,k} \end{pmatrix} = T_2 \begin{pmatrix} d_{2,1,A,k} \\ a_{-1,k} \end{pmatrix}, \tag{17}$$

with

$$T_i = \begin{pmatrix} \dfrac{E}{t_{\mathrm{R},i}} & -\dfrac{\upsilon_i}{t_{\mathrm{R},i}} \\ 1 & 0 \end{pmatrix} [M_i]^{N_i - 1} \begin{pmatrix} \dfrac{E}{\upsilon_i} & -\dfrac{t_{\mathrm{L},i}}{\upsilon_i} \\ 1 & 0 \end{pmatrix},$$
$$M_i = \begin{pmatrix} \dfrac{E}{\upsilon_i} & -\dfrac{w}{\upsilon_i} \\ 1 & 0 \end{pmatrix} \begin{pmatrix} \dfrac{E}{w} & -\dfrac{\upsilon_i}{w} \\ 1 & 0 \end{pmatrix}.$$

Moreover, Eqs. (16) and (17) can be further written as

$$a_{1,k} = [T_1]_{11} d_{1,1,A,k} + [T_1]_{12} a_{-1,k}, \tag{18}$$
$$d_{1,N_1,B,k} = [T_1]_{21} d_{1,1,A,k} + [T_1]_{22} a_{-1,k}, \tag{19}$$
$$a_{1,k} = [T_2]_{11} d_{2,1,A,k} + [T_2]_{12} a_{-1,k}, \tag{20}$$
$$d_{2,N_2,B,k} = [T_2]_{21} d_{2,1,A,k} + [T_2]_{22} a_{-1,k}. \tag{21}$$

To simplify the calculation, the wave functions associated with the conduction electrons are chosen as plane waves, and the corresponding wave amplitudes of the left and right leads read as

$$\begin{aligned} a_{-1,k} &= \mathrm{e}^{-\mathrm{i}ka} + r_{\text{reflection}}\mathrm{e}^{\mathrm{i}ka}, \\ a_{-2,k} &= \mathrm{e}^{-2\mathrm{i}ka} + r_{\text{reflection}}\mathrm{e}^{2\mathrm{i}ka}, \end{aligned} \tag{22}$$
$$\begin{aligned} a_{1,k} &= t_{\text{transmission}}\mathrm{e}^{\mathrm{i}ka}, \\ a_{2,k} &= t_{\text{transmission}}\mathrm{e}^{2\mathrm{i}ka}. \end{aligned} \tag{23}$$

Then, inserting Eqs. (22) and (23) into Eqs. (6), (18)–(21), and (15), the six coupled linear equations can be rewritten as

$$\begin{aligned} -[T_1]_{12}\mathrm{e}^{-\mathrm{i}ka} &= [T_1]_{12}\mathrm{e}^{\mathrm{i}ka} r_{\text{reflection}} + [T_1]_{11} d_{1,1,A,k} \\ &\quad - \mathrm{e}^{\mathrm{i}ka} t_{\text{transmission}}, \\ -[T_1]_{22}\mathrm{e}^{-\mathrm{i}ka} &= [T_1]_{22}\mathrm{e}^{\mathrm{i}ka} r_{\text{reflection}} + [T_1]_{21} d_{1,1,A,k} \\ &\quad - d_{1,N_1,B,k}, \\ -[T_2]_{12}\mathrm{e}^{-\mathrm{i}ka} &= [T_2]_{12}\mathrm{e}^{\mathrm{i}ka} r_{\text{reflection}} + [T_2]_{11} d_{2,1,A,k} \\ &\quad - \mathrm{e}^{\mathrm{i}ka} t_{\text{transmission}}, \\ -[T_2]_{22}\mathrm{e}^{-\mathrm{i}ka} &= [T_2]_{22}\mathrm{e}^{\mathrm{i}ka} r_{\text{reflection}} + [T_2]_{21} d_{2,1,A,k} \\ &\quad - d_{2,N_2,B,k}, \\ E\mathrm{e}^{-\mathrm{i}ka} - t_0\mathrm{e}^{-2\mathrm{i}ka} &= \left(t_0\mathrm{e}^{2\mathrm{i}ka} - E\mathrm{e}^{\mathrm{i}ka}\right) r_{\text{reflection}} \\ &\quad + t_{\mathrm{L},1} d_{1,1,A,k} + t_{\mathrm{L},2} d_{2,1,A,k}, \\ 0 &= t_{\mathrm{R},1} d_{1,N_1,B,k} + t_{\mathrm{R},2} d_{2,N_2,B,k} \\ &\quad + \left(t_0\mathrm{e}^{2\mathrm{i}ka} - E\mathrm{e}^{\mathrm{i}ka}\right) t_{\text{transmission}}. \end{aligned}$$

By solving the above coupled linear equations, the transmission probability of electron through the ring-shaped SSH double-chain system is given by

$$T = |t_{\text{transmission}}|^2.$$

3. Results and discussion

We now study the transmission probabilities of electron transport through the ring-shaped SSH double-chain system in the vicinity of the zero energy. In the following numerical calculations, the parameters of the ring-shaped SSH double-chain system are chosen as $t_{\mathrm{L},1} = t_{\mathrm{L},2} = t_{\mathrm{L}}$, $t_{\mathrm{R},1} = t_{\mathrm{R},2} = t_{\mathrm{R}}$, $t_{\mathrm{L}} = t_{\mathrm{R}} = t$, $t_0 = 1.0$, and $w = 1.0$. To investigate electron transport signatures of the non-trivial edge states in the ring-shaped SSH double-chain, we first discuss the SSH single-chain system.

3.1. The topological properties of the SSH single-chain

In a finite-length SSH single-chain, the energy difference between the two non-trivial topological edge states is not equal to zero, which depends on the intra-cell hopping amplitude υ, see Fig. 2(a). Moreover, for a given intra-cell hopping amplitude υ, the energy difference between the two non-trivial topological edge states depends on the length of SSH single-chain, namely, the number of cells N, see Fig. 2(b). To characterize the non-trivial topological properties of the SSH single-chain, we here choose the winding number to describe the non-trivial topological edge states. For a infinite SSH single-chain, the winding number of non-trivial topological edge states is equal to 1 when $\upsilon < w$.[37] However, the non-trivial topological region of a finite-length SSH single-chain is smaller than the above mentioned prediction region. Taking into account the inter-cell hopping amplitude $w = 1.0$, we set $\upsilon \leq 0.5$ when considering the SSH single-chain being of non-trivial topological edge states.

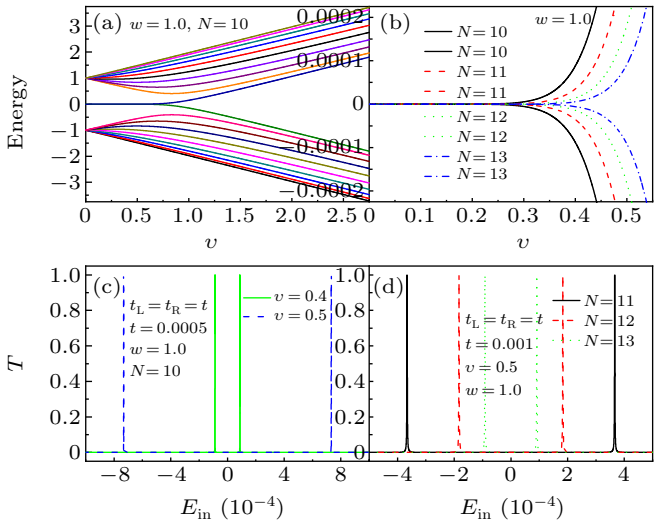


Fig. 2. (a) The energy spectrum of the finite-length SSH single-chain with $N = 10$. (b) The energy spectrum of the non-trivial topological edge states for different finite-length SSH single-chain. (c) and (d) The transmission probabilities of electron transport through the SSH single-chain in the vicinity of the zero energy as a function of the energy of incident electron. (c) The same finite-length SSH single-chain for different intra-cell hopping amplitudes with $N = 10$ and $t_L = t_R = 0.0005$. (d) The different finite-length SSH single-chain with $\upsilon = 0.5$ and $t_L = t_R = 0.001$. The inter-cell hopping amplitude of the SSH single-chain is chosen as $w = 1.0$.

To explore the dependence of the non-trivial topological edge states of the SSH single-chain on the electron transport properties, we study the electron transport through the finite-length SSH single-chain in the vicinity of the zero energy. When the SSH single-chain weakly coupled to the source and drain leads, the positions of transmission resonance peaks in the vicinity of the zero energy can characterize the energy spectrum of the non-trivial topological edge states, see Figs. 2(c) and 2(d). Consequently, the properties of transmission resonance peaks associated with the non-trivial topological edge states suggest an alternative scheme to determine whether the SSH single-chain is of the non-trivial topological edge states or not.

3.2. Detecting non-trivial topological edge states of the SSH single-chain

In general, to detect the non-trivial topological edge states of the SSH single-chain based on the properties of transmission resonance peaks in the vicinity of the zero energy, it is necessary to study the signatures of transmission resonance peaks associated with the non-trivial topological edge states as a function of the externally tunable physical quantities. Here, we select the strength of tunneling coupling between the SSH single-chain and the two leads $t_L = t_R$ as a tunable physical quantity. In the case of the SSH single-chain weakly coupled to the source and drain leads, e.g., $t_L = t_R = 0.004$, the transmission probability of the SSH single-chain in the vicinity of the zero energy displays the two resonance peaks, see the solid line in Fig. 3(a). With increasing the tunneling coupling strength $t_L = t_R$, the two transmission resonance peaks first evolved into a relatively wide resonance peak gradually, and then the wide resonance peak disappears finally when the tunneling coupling strength $t_L = t_R$ reaches a certain value, e.g., $t_L = t_R = 0.05$, see Fig. 3(a). We next illustrate the physical mechanism of electron transport properties of the SSH single-chain in the vicinity of the zero energy.

In the case of the SSH single-chain coupled to the two leads, the energy spectrum of the SSH single-chain will be influenced by the electron tunneling processes between the SSH single-chain and the two leads. To understand the dependence of the energy spectrum of the SSH single-chain on the magnitude of the tunneling coupling strength, we here consider the energy spectrum of the SSH single-chain coupled to the two nearest-neighbor lattices of the left and right leads $j = -1$ and $j = 1$. When the SSH single-chain weakly coupled to the two leads, the magnitude of the tunneling coupling strength has a slight influence on the energy spectrum of the SSH single-chain. Consequently, the positions of the two transmission resonance peaks in the vicinity of the zero energy correspond to the energy levels of the two non-trivial topological edge states, see the solid lines in Fig. 3(b). However, the magnitude of the tunneling coupling strength will have a significant influence on the energy spectrum of the SSH single-chain when the SSH single-chain strongly coupled to the two leads. Particularly, the energy levels of the two non-trivial topological edge states will disappear, see the dashed lines in Fig. 3(b), as a results the transmission probability approaches zero, see the short-dash-dotted line in Fig. 3(a). Therefore, the number of transmission resonance peaks associated with the non-trivial topological edge states will be reduced from two to zero with increasing the strength of tunneling coupling between the SSH single-chain and the two leads from the weak to the strong

coupling regimes. These results suggest an alternative way to detect whether the SSH single-chain is of the non-trivial topological edge states or not.

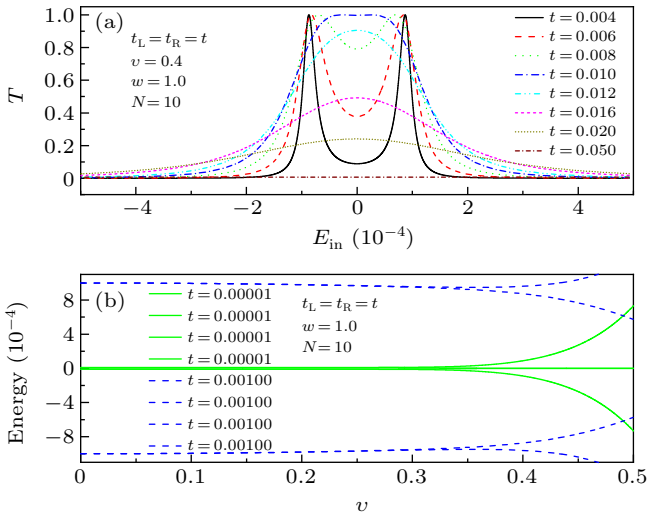


Fig. 3. (a) The transmission probabilities of electron transport through the SSH single-chain in the vicinity of the zero energy as a function of the energy of incident electron for different strengths of tunneling coupling $t_L = t_R$. (b) Energy spectrum of the SSH single-chain coupled to the two nearest-neighbor lattices of the left and right leads $j = -1$ and $j = 1$ in the vicinity of the zero energy with $t_L = t_R = 0.00001$ and $t_L = t_R = 0.001$. The parameters of the SSH single-chain are chosen as $\upsilon = 0.4$, $w = 1.0$, and $N = 10$.

3.3. Detecting non-trivial topological edge states of ring-shaped SSH double-chain

In a ring-shaped SSH double-chain system, the conduction electrons from the source electrode have two different paths of the upper and lower chains tunnel out the SSH system and tunnel into the drain electrode finally. Consequently, we can study the influence of the quantum interference between the two different electron tunneling paths on the electron transport properties of the non-trivial topological edge states. Here, we discuss the two cases, namely, the ring-shaped SSH double-chain with the upper chain being different from the lower one, and that with the upper chain being the same as the lower one. In the former case, we consider the two types of ring-shaped SSH double-chain, namely, the length of upper chain being the same as the lower one but with different intra-cell hopping amplitude, and the intra-cell hopping amplitude of the upper chain being the same as the lower one but with different length.

In the first type of ring-shaped SSH double-chain with the upper chain being different from the lower one, we choose $\upsilon_1 = 0.4$, $\upsilon_2 = 0.5$, and $N_1 = N_2 = 10$. When the ring-shaped SSH double-chain weakly coupled to the two leads, the transmission probability displays the four resonance peaks in the vicinity of the zero energy, see the solid and the dashed lines in Fig. 4(a). Here, the positions of the two middle resonance peaks correspond to that of two resonance peaks of the SSH single-chain with $\upsilon = 0.4$, while the positions of the two other resonance peaks correspond to that of two resonance peaks of the SSH single-chain with $\upsilon = 0.5$. When the tunneling coupling strength $t_L = t_R$ is increased gradually, the width of the four resonance peaks will be broadened, and the positions of the first peak on the left and that of the first peak on the right will move towards the zero energy position, and the two middle resonance peaks will especially evolve into a relatively wide resonance peak, see Fig. 4(b). Interestingly, when the tunneling coupling strength $t_L = t_R$ reaches at a certain value, the width of the first peak on the left and that of the first peak on the right will become narrower and form two sharp peaks finally, whereas the relatively wide resonance peak evolved from the two middle resonance peaks will disappear gradually, see Fig. 4(c).

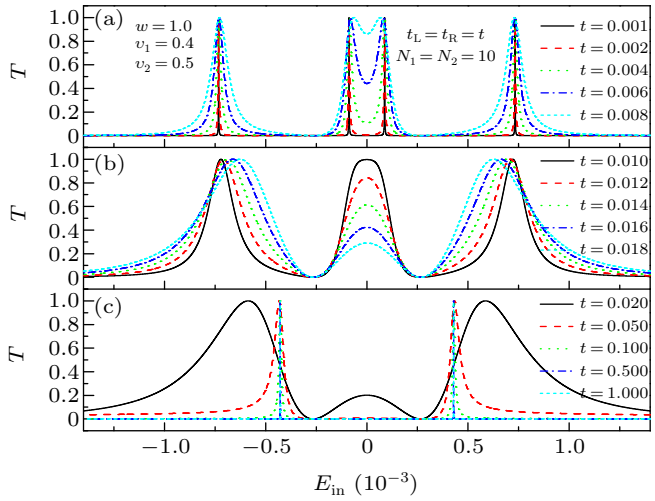


Fig. 4. The transmission probabilities of electron transport through the ring-shaped SSH double-chain in the vicinity of the zero energy as a function of the energy of incident electron for different strengths of tunneling coupling $t_L = t_R$. The parameters of the ring-shaped SSH double-chain are chosen as $\upsilon_1 = 0.4$, $\upsilon_2 = 0.5$, $w = 1.0$, and $N_1 = N_2 = 10$.

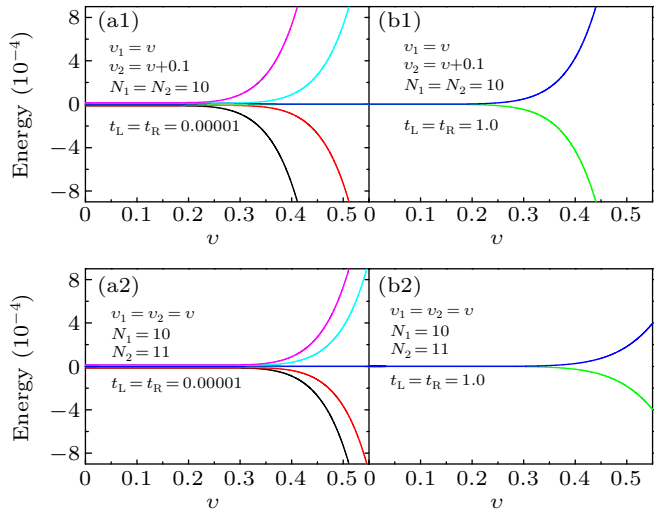


Fig. 5. Energy spectrum of the ring-shaped SSH double-chain coupled to the two nearest-neighbor lattices of the left and right leads $j = -1$ and $j = 1$ in the vicinity of the zero energy with $w = 1.0$. (a1) $t_L = t_R = 0.00001$ and $N_1 = N_2 = 10$. (b1) $t_L = t_R = 1.0$ and $N_1 = N_2 = 10$. (a2) $t_L = t_R = 0.00001$, $N_1 = 10$ and $N_2 = 11$. (b2) $t_L = t_R = 1.0$, $N_1 = 10$ and $N_2 = 11$.

To illustrate the physical mechanism of the transmission resonance peaks, we also consider the energy spectrum of

the ring-shaped SSH double-chain coupled to the two nearest-neighbor lattices of the left and right leads $j = -1$ and $j = 1$. In the weak coupling regime, e.g., $t_L = t_R = 0.00001$, the four energy levels in the vicinity of the zero energy correspond to the positions of the four transmission resonance peaks, see Figs. 4(a) and 5(a1). Whereas in the strong coupling regime, e.g., $t_L = t_R = 1.0$, the two energy levels in the vicinity of the zero energy correspond to the positions of the two transmission resonance peaks, see Figs. 4(c) and 5(b1), which is different from the case of the SSH single-chain. To further determine that whether the eigenstates of these energy levels in the vicinity of the zero energy is of the non-trivial topological edge states or not, it is necessary to investigate the distribution of probability amplitudes of the wave functions of these nearly zero-energy eigenstates. In the weak coupling regime, the distribution of probability amplitudes of the wave functions of the four nearly zero-energy eigenstates display the characteristics of non-trivial topological edge states, namely, the first and last sublattices of the upper and lower chains have the maximum magnitudes of probability amplitudes, respectively, and the magnitude of the probability amplitudes exponentially decays from the two ends to the middle of the upper (lower) chain, see Figs. 6(a1)–6(d1). While in the strong coupling regime, the wave functions of the two nearly zero-energy eigenstates are also exponentially localized at the two ends of the upper and lower chains, see Figs. 7(a1) and 7(b1). This characteristic indicates that the first type of ring-shaped SSH double-chain strongly coupled to the two leads still has two non-trivial topological edge states.

While in the second type of ring-shaped SSH double-chain, we choose $\upsilon_1 = \upsilon_2 = 0.5$, $N_1 = 10$, and $N_2 = 11$. In the vicinity of the zero energy, with increasing the tunneling coupling strength from the weak to the strong coupling regimes, the variation of the transmission resonance peaks is the same as that in the first type of ring-shaped SSH double-chain, see Fig. 8. Moreover, the positions of the transmission resonance peaks in the weak and strong coupling regimes also correspond to the energy levels of the ring-shaped SSH double-chain coupled to the two nearest-neighbor lattices of the left and right leads $j = -1$ and $j = 1$, see Figs. 8, 5(a2), and 5(b2). Importantly, the wave functions of the four nearly zero-energy eigenstates in the weak coupling regime and that of the two nearly zero-energy eigenstates in the strong coupling regime are also exponentially localized at the two ends of the upper and lower chains, see Figs. 6(a2)–6(d2), 7(a2), and 7(b2). Consequently, the second type of ring-shaped SSH double-chain in the weak and strong coupling regimes also has the four and two non-trivial topological edge states, respectively.

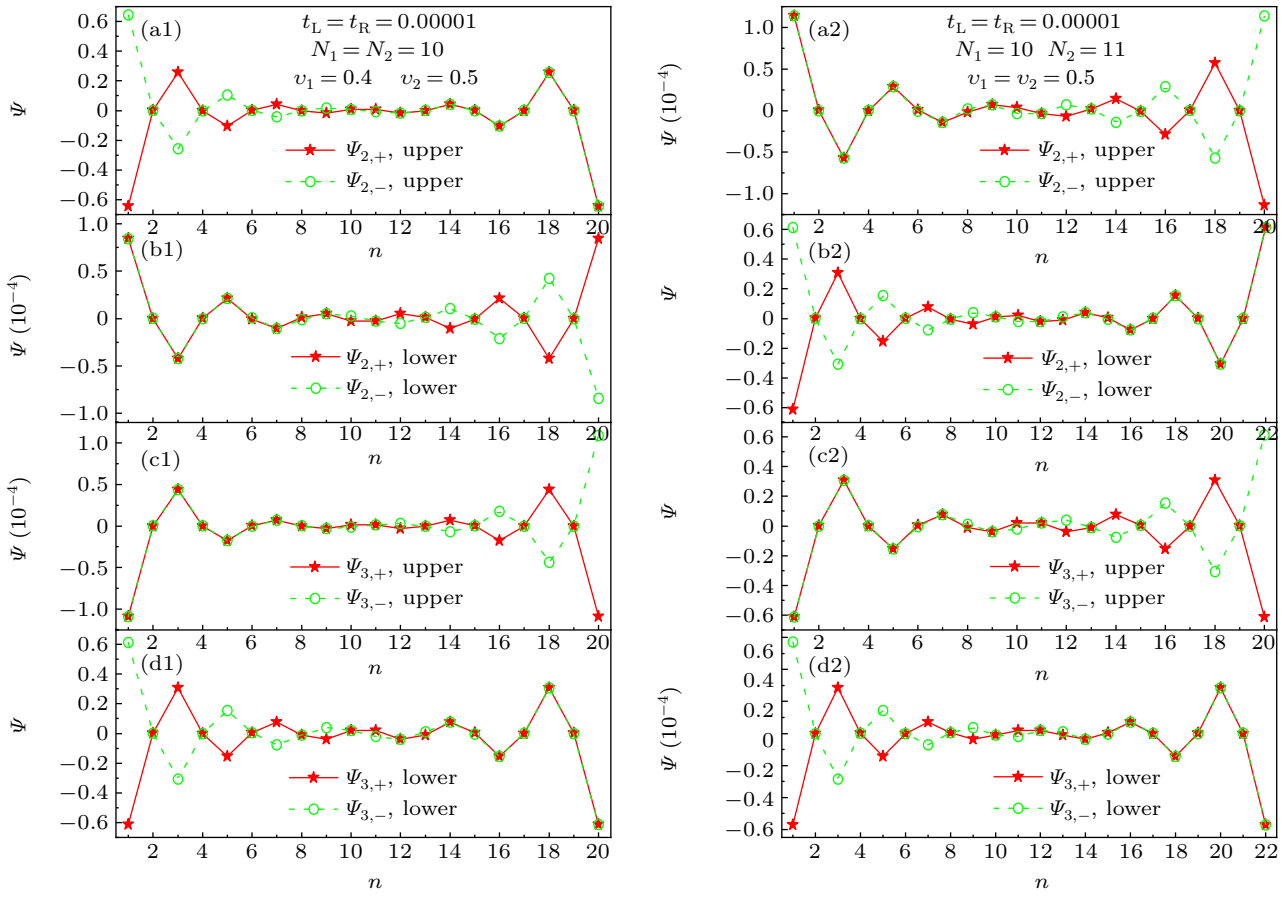


Fig. 6. The distribution of probability amplitudes of the wave functions of the four nearly zero-energy eigenstates of the ring-shaped SSH double-chain coupled to the two nearest-neighbor lattices of the left and right leads $j = -1$ and $j = 1$ with $w = 1.0$ and $t_L = t_R = 0.00001$. (a1)–(d1), $\upsilon_1 = 0.4$, $\upsilon_2 = 0.5$, and $N_1 = N_2 = 10$. (a2)–(d2), $\upsilon_1 = \upsilon_2 = 0.5$, $N_1 = 10$, and $N_2 = 11$.

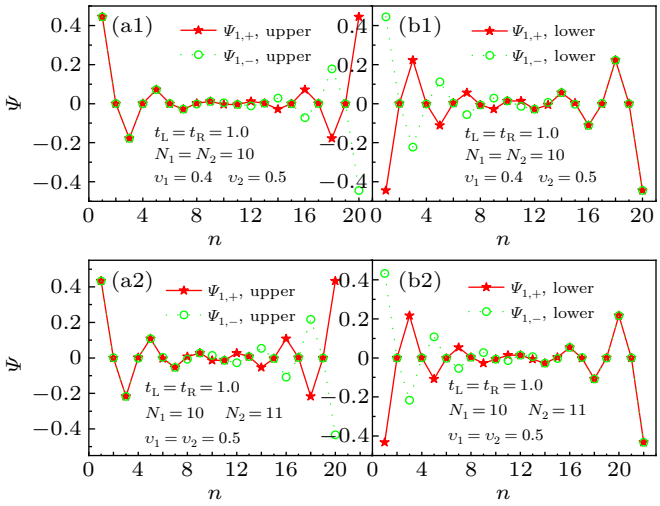


Fig. 7. The distribution of probability amplitudes of the wave functions of the two nearly zero-energy eigenstates of the ring-shaped SSH double-chain coupled to the two nearest-neighbor lattices of the left and right leads $j = -1$ and $j = 1$ with $w = 1.0$ and $t_L = t_R = 1.0$. (a1) and (b1) $\upsilon_1 = 0.4$, $\upsilon_2 = 0.5$, and $N_1 = N_2 = 10$. (a2) and (b2) $\upsilon_1 = \upsilon_2 = 0.5$, $N_1 = 10$, and $N_2 = 11$.

We last discuss the case of the upper chain being the same as the lower one, and choose $\upsilon_1 = \upsilon_2 = 0.4$ and $N_1 = N_2 = 10$. In the vicinity of the zero energy, the transmission probability in the weak coupling regime displays the two resonance peaks only, see Fig. 9(a), which is different from the case of the upper chain being different from the lower one, see Figs. 4(a) and 8(a). Particularly, the two transmission resonance peaks will disappear gradually by increasing the tunneling coupling strength from the weak to the strong coupling regimes, see Fig. 9(a). These characteristics can also be understood in terms of the energy spectrum of the ring-shaped SSH double-chain coupled to the two nearest-neighbor lattices of the left and right leads $j = -1$ and $j = 1$. In the weak coupling regime, the energy spectrum of the system have the two twofold-degenerate energy levels in the vicinity of the zero energy, see the dashed and the dotted lines Fig. 9(b), thus the two corresponding transmission resonance peaks is found. Whereas in the strong coupling regime, although the energy spectrum of the system has two non-degenerate energy levels in the vicinity of the zero energy, see the dash-dotted lines Fig. 9(b), the transmission resonance peak can not found. This characteristic indicates that the disappearance mechanism of the transmission resonance peaks can be attributed to the destructive interference between the two different electron tunneling paths of the upper and lower chains.

Therefore, in the ring-shaped SSH double-chain coupled to the two leads, with increasing the tunneling coupling strength from the weak to the strong coupling regimes, the number of transmission resonance peaks in the vicinity of the zero energy will be reduced by two. For example, in the case of the upper chain being different from the lower one, the number of transmission resonance peaks will be reduced from four to two; whereas that will be reduced from two to zero in the case of the upper chain being the same as the lower one. These results suggest an alternative way to detect whether the ring-shaped SSH double-chain system is of the non-trivial topological edge states or not.

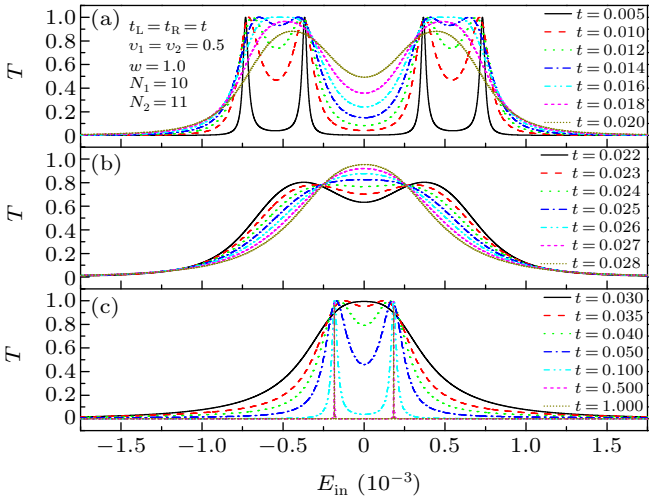


Fig. 8. The transmission probabilities of electron transport through the ring-shaped SSH double-chain in the vicinity of the zero energy as a function of the energy of incident electron for different strengths of tunneling coupling $t_L = t_R$. The parameters of the ring-shaped SSH double-chain are chosen as $\upsilon_1 = \upsilon_2 = 0.5$, $w = 1.0$, $N_1 = 10$, and $N_2 = 11$.

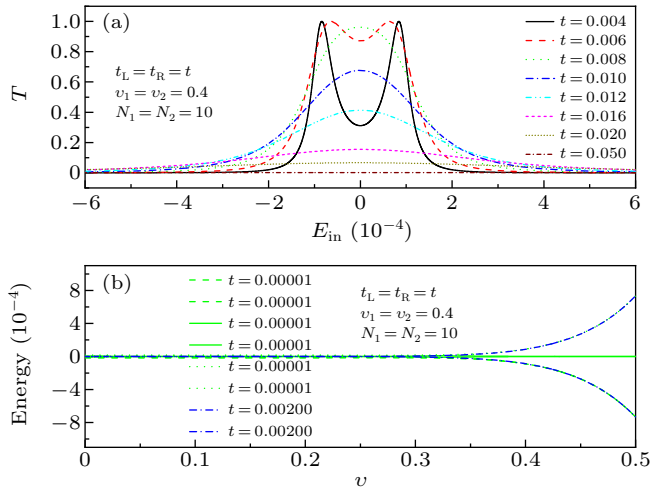


Fig. 9. (a) The transmission probabilities of electron transport through the ring-shaped SSH double-chain in the vicinity of the zero energy as a function of the energy of incident electron for different strengths of tunneling coupling $t_L = t_R$. (b) Energy spectrum of the ring-shaped SSH double-chain coupled to the two nearest-neighbor lattices of the left and right leads $j = -1$ and $j = 1$ with $t_L = t_R$. The parameters of the ring-shaped SSH double-chain system are chosen as $\upsilon_1 = \upsilon_2 = 0.4$, $w = 1.0$, and $N_1 = N_2 = 10$.

4. Conclusion

We have studied the transmission probability of electron transport through the ring-shaped SSH double-chain system in the vicinity of the zero energy. We have demonstrated that the positions of transmission resonance peaks in the vicinity of the zero energy correspond to the energy levels of the non-trivial topological edge states. In particular, the quantum interference between the two different electron tunneling paths of the upper and lower chains has a significant influence on the num-

ber of transmission resonance peaks associated with the non-trivial topological edge states. For example, in the case of the upper chain being different from the lower one, the electron transmission probability displays the four and two resonance peaks in the weak and strong coupling regimes, respectively; whereas in the case of the upper chain being the same as the lower one, the electron transmission probability displays the two transmission resonance peaks in the weak coupling regime only, and the transmission resonance peak disappears in the strong coupling regime that originated from the destructive interference between the two different electron tunneling paths of the upper and lower chains. The predicted properties of the variation of the number of transmission resonance peaks associated with the non-trivial topological edge states in the weak and strong coupling regimes suggest an alternative way to detect whether the ring-shaped SSH double-chain system is of the non-trivial topological edge states or not.

Acknowledgments

Project supported by the National Natural Science Foundation of China (Grant No. 11974153), the Natural Science Foundation of Shanxi Province, China (Grant No. 20210302123184), the Program for the Outstanding Innovative Teams of Higher Learning Institutions of Shanxi Province, China (Grant No. 163220120-S), and the Natural Science Foundation of Shandong Province, China (Grant No. ZR2020MA091).

References

[1] Moore J E 2010 *Nature* **464** 194
[2] Hasan M Z and Kane C L 2010 *Rev. Mod. Phys.* **82** 3045
[3] Su W P, Schrieffer J R and Heeger A J 1979 *Phys. Rev. Lett.* **42** 1698
[4] Naz E S G, Fulga I C, Ma L, Schmidt O G and van den Brink J 2018 *Phys. Rev. A* **98** 033830
[5] Whittaker C E, Cancellieri E, Walker P M, Royall B, Rodriguez L E T, Clarke E, Whittaker D M, Schomerus H, Skolnick M S and Krizhanovskii D N 2019 *Phys. Rev. B* **99** 081402
[6] Wang Y, Lu Y H, Mei F, Gao J, Li Z M, Tang H, Zhu S L, Jia S and Jin X M 2019 *Phys. Rev. Lett.* **122** 193903
[7] Atala M, Aidelsburger M, Barreiro J T, Abanin D, Kitagawa T, Demler E and Bloch I 2013 *Nat. Phys.* **9** 795
[8] Drost R, Ojanen T, Harju A and Liljeroth P 2017 *Nat. Phys.* **13** 668
[9] Huda M N, Kezilebieke S, Ojanen T, Drost R and Liljeroth P 2020 *npj Quantum Mater.* **5** 17
[10] Parto M, Wittek S, Hodaei H, Harari G, Bandres M A, Ren J, Rechtsman M C, Segev M, Christodoulides D N and Khajavikhan M 2018 *Phys. Rev. Lett.* **120** 113901
[11] Ryu S and Hatsugai Y 2002 *Phys. Rev. Lett.* **89** 077002
[12] Hafezi M 2014 *Phys. Rev. Lett.* **112** 210405
[13] Li L, Xu Z and Chen S 2014 *Phys. Rev. B* **89** 085111
[14] Poshakinskiy A V, Poddubny A N and Hafezi M 2015 *Phys. Rev. A* **91** 043830
[15] Marques A M and Dias R G 2017 *Phys. Rev. B* **95** 115443
[16] Li C, Lin S, Zhang G and Song Z 2017 *Phys. Rev. B* **96** 125418
[17] Padavić K, Hegde S S, DeGottardi W and Vishveshwara S 2018 *Phys. Rev. B* **98** 024205
[18] Li C F, Li X P and Wang L C 2018 *Europhys. Lett.* **124** 37003
[19] Lu M X and Deng W J 2019 *Acta Phys. Sin.* **68** 120301 (in Chinese)
[20] Lü X L and Xie H 2019 *J. Phys.: Condens. Matter* **31** 495401
[21] Pérez-González B, Bello M, Platero G and Gómez-León Á 2019 *Phys. Rev. Lett.* **123** 126401
[22] Du L, Wu J H, Artoni M and Rocca G C L 2019 *Phys. Rev. A* **100** 012112
[23] Simon D S, Osawa S and Sergienko A V 2019 *J. Phys.: Condens. Matter* **31** 045001
[24] Benito M, Niklas M, Platero G and Kohler S 2016 *Phys. Rev. B* **93** 115432
[25] Balabanov O and Johannesson H 2020 *J. Phys.: Condens. Matter* **32** 015503
[26] Dong B and Lei X L 2018 *Ann. Physics* **396** 245
[27] Niklas M, Benito M, Kohler S and Platero G 2016 *Nanotechnology* **27** 454002
[28] Böhling S, Engelhardt G, Platero G and Schaller G 2018 *Phys. Rev. B* **98** 035132
[29] Zhang L Y, Xue H B, Chen B, Chen J B and Xing L L 2020 *Acta Phys. Sin.* **69** 077301 (in Chinese)
[30] Xue H B, Duan Z L, Chen B, Chen J B and Xing L L 2021 *Acta Phys. Sin.* **70** 087301 (in Chinese)
[31] Bartolo T C, Smith J S, Muralidharan B, Müller C, Stace T M and Cole J H 2020 *Phys. Rev. Research* **2** 043430
[32] Gou W, Chen T, Xie D, Xiao T, Deng T S, Gadway B, Yi W and Yan B 2020 *Phys. Rev. Lett.* **124** 070402
[33] Haug T, Dumke R, Kwek L C and Amico L 2019 *Commun. Phys.* **2** 127
[34] Marques A M and Dias R G 2018 *J. Phys.: Condens. Matter* **30** 305601
[35] Xue H B, Zhang H Y, Nie Y H, Li Z J and Liang J Q 2010 *Chin. Phys. B* **19** 047303
[36] Chakrabarti A, Römer R A and Schreiber M 2003 *Phys. Rev. B* **68** 195417
[37] Asbóth J K, Oroszlány L and Pályi A 2016 *A Short Course on Topological Insulators* (Budapest: Springer)